Phase Behavior and Thermal Properties of Ternary Ionic Liquid−Lithium Salt (IL−IL−LiX) Electrolytes

Qian Zhou,[†] Wesley A. Henderson,*[,†] Giovanni B. Appetecchi,[‡] and Stefano Passerini*[,‡,§]

ILEET (Ionic Liquids and Electrolytes for Energy Technologies) Laboratory, Department of Chemical & Biomolecular Engineering, North Carolina State University, Raleigh, North Carolina 27695, Italian National Agency for New Technologies, Energy, and Sustainable Economic Development (ENEA), IDROCOMB, Via Anguillarese 301, 00123 Rome, Italy, and Institute of Physical Chemistry, University of Muenster, Muenster D 48149, Germany

Received: December 12, 2009; Revised Manuscript Received: February 7, 2010

The phase behavior and thermal properties of ternary ionic liquid−lithium salt (IL−IL−LiX) mixtures intended for use as electrolytes for lithium batteries are reported here. It is shown that the addition of small amounts of *N*-methyl-*N*-propylpyrrolidinium bis(fluorosulfonyl)imide ($PY_{13}FSI$) to *N*-butyl-*N*-methylpyrrolidinium bis(trifluoromethanesulfonyl)imide ($PY_{14}TFSI$)−lithium salt (LiTFSI or $LiPF_6$) mixtures greatly hinders the ability of the samples to crystallize. This results in a much improved subambient temperature conductivity for the mixtures relative to the binary IL−LiX electrolytes at low temperature. The thermal stability of the mixtures is reduced by the addition of $PY_{13}FSI$ but remains acceptable for Li battery applications.

Introduction

State-of-the-art lithium battery liquid electrolytes consist of mixtures of aprotic solvents with a lithium salt (i.e., $LiPF_6$).[1] The solvents are mixed together to achieve a synergic beneficial effect on the electrolyte characteristics and properties. There is considerable interest in replacing the currently used aprotic solvents with ionic liquids (ILs).[2–13] ILs are salts, or mixtures of salts, which melt at low temperature and are therefore liquids composed solely of ions. The unique characteristics of ILs make them potentially excellent materials for battery electrolytes, but to date, no single IL has been found with optimal properties for this application.[14,15] For example, $PY_{1R}TFSI$−LiTFSI electrolytes are known to have excellent electrochemical and thermal stability, but also have a relatively low ionic conductivity, high viscosity, tend to solidify into crystalline phases,[16] and do not form a solid electrolyte interface (SEI) layer with graphite.[17] In contrast, $PY_{1R}FSI$−LiFSI mixtures have a higher conductivity, lower viscosity, form an excellent SEI layer on graphite, and remain amorphous rather than crystallizing, but they also suffer from a much lower thermal stability.[18,19]

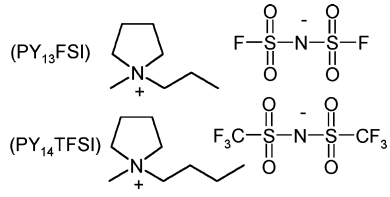

In this article, the thermal properties of $PY_{13}FSI$−$PY_{14}TFSI$−LiTFSI and $PY_{13}FSI$−$PY_{14}TFSI$−$LiPF_6$ mixtures are explored to further characterize the favorable properties of the two ILs as electrolytes for Li batteries, especially at subambient temperatures. $PY_{13}FSI$ exhibits a low viscosity and a low T_m (−9 °C) with a high conductivity (6.4 mS cm^{-1}) at room temperature.[18] The electrolyte formed by dissolving LiTFSI in $PY_{13}FSI$ was reported to allow reversible lithium insertion/deinsertion in graphite electrodes.[17] However, $PY_{13}FSI$ has a lower thermal and electrochemical stability than $PY_{14}TFSI$. $PY_{14}TFSI$ and its mixtures with lithium salts have a reasonable room-temperature ionic conductivity (>1 mS cm^{-1}) and an overall electrochemical stability window in excess of 5.5 V with the cathodic stability limit exceeding the lithium plating/stripping potential.[20] $LiPF_6$ was selected because of its wide use and favorable properties. LiTFSI was also selected for comparison purposes to investigate the effect of the PF_6^- anions ($TFSI^-$ anions are already present in the system). The LiX (i.e., LiTFSI or $LiPF_6$) concentration was fixed at 0.3 M based upon preliminary battery cycling test results obtained on carbonaceous anodes.[17,21] These ternary electrolytes were shown to have conductivity increases at very low temperatures (from −20 to −40 °C) of up to 3 orders of magnitude with respect to the binary IL−LiX mixtures.[17]

Experimental Methods

Sample Preparation. The $PY_{14}TFSI$ and $PY_{13}FSI$ ILs were synthesized and dried as previously reported.[17,20] The binary IL electrolyte mixtures with LiX ($LiPF_6$ or LiTFSI) were prepared by combining the appropriate amounts of the salts in vials and stirring. Table 1 indicates the mole composition of the mixtures. The materials were stored in hermetically sealed glass vials in a controlled environment (either a dry room, RH < 0.1% at 20 °C, or a N_2 glovebox with <5 ppm H_2O).

Thermal Measurements. DSC measurements were performed using a TA Instruments Q2000 differential scanning calorimeter with liquid N_2 cooling. The instrument was calibrated with cyclohexane (solid−solid phase transition at −87.06 °C; melt transition at 6.54 °C) and indium (melt transition at 156.60 °C). Hermetically sealed Al pans were prepared in the glovebox. Typically, sample pans were slowly

* To whom correspondence should be addressed. E-mail: whender@ncsu.edu (W.A.H.); stefano.passerini@uni-muenster.de (S.P.).
† North Carolina State University.
‡ ENEA.
§ University of Muenster.

10.1021/jp911759d
Published on Web 03/17/2010

TABLE 1: Mole Composition of $(1 - x)$ $PY_{14}TFSI-(x)PY_{13}FSI-0.3$ M LiX Mixtures (X = $TFSI^-$ or PF_6^-)[a]

$PY_{13}FSI$		$PY_{14}TFSI$	
mole fraction	weight fraction	mole fraction	weight fraction
0	0	1	1.00
0.067	0.05	0.933	0.95
0.132	0.10	0.868	0.90
0.255	0.20	0.745	0.80
0.370	0.30	0.630	0.70
0.477	0.40	0.523	0.60
0.578	0.50	0.422	0.50
1	1.00	0	0

[a] The parameters x and $(1 - x)$ are the mole fractions of $PY_{13}FSI$ and $PY_{14}TFSI$, respectively.

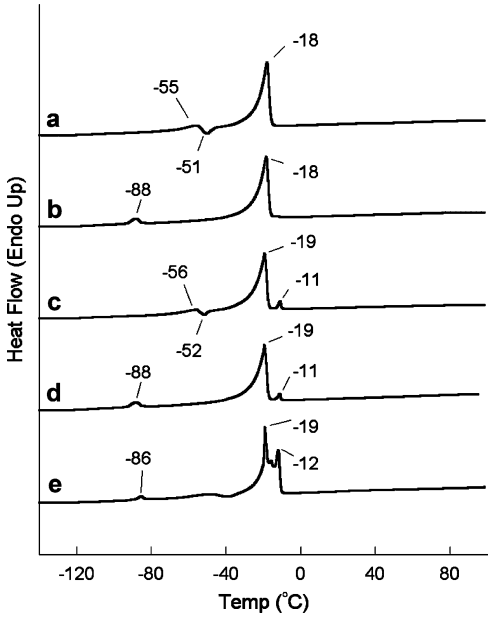

Figure 1. DSC heating traces (5 °C min^{-1}) of $PY_{13}FSI$-0.3 M $LiPF_6$. The sample was (a) cooled to −150 °C and heated to 100 °C, (b) annealed at −50 °C for 10 min, cooled to −60 °C, annealed at −50 °C for 10 min, cooled to −150 °C and heated to 100 °C, (c) cooled to −150 °C and heated to 100 °C, (d) cooled to −150 °C, annealed at −50 °C for 10 min, cooled to −150 °C and heated to 100 °C and (e) cooled to −150 °C, annealed at −65 °C for 10 min, cooled to −150 °C and heated to 100 °C.

cooled (5 °C min^{-1}) to −150 °C and then heated (5 °C min^{-1}) to 100 °C. In some cases, it was necessary to hold or cycle the samples extensively at various subambient temperatures in the instrument prior to the measurements to ensure complete crystallization (where possible). Peak temperatures are reported for the endotherms and exotherms.

TGA measurements were performed using a TA Instruments Q5000 thermogravimetric analyzer. The thermal stability was analyzed by heating from ambient temperature to 600 °C under a N_2 atmosphere (>99.99%, water concentration 2−5 ppm).

Results and Discussion

Interestingly, there is some significant variation in the DSC heating traces for the same $PY_{13}FSI$−0.3 M $LiPF_6$ sample (Figure 1) when various thermal cycling procedures (not shown) are used for crystallization. The pure $PY_{13}FSI$ IL crystallizes with a T_m of −9 °C; prior to this, however, this salt also undergoes solid−solid phase transitions at −83 and −19 °C.[18] Another peak was found for the pure $PY_{13}FSI$ salt at −50 °C,

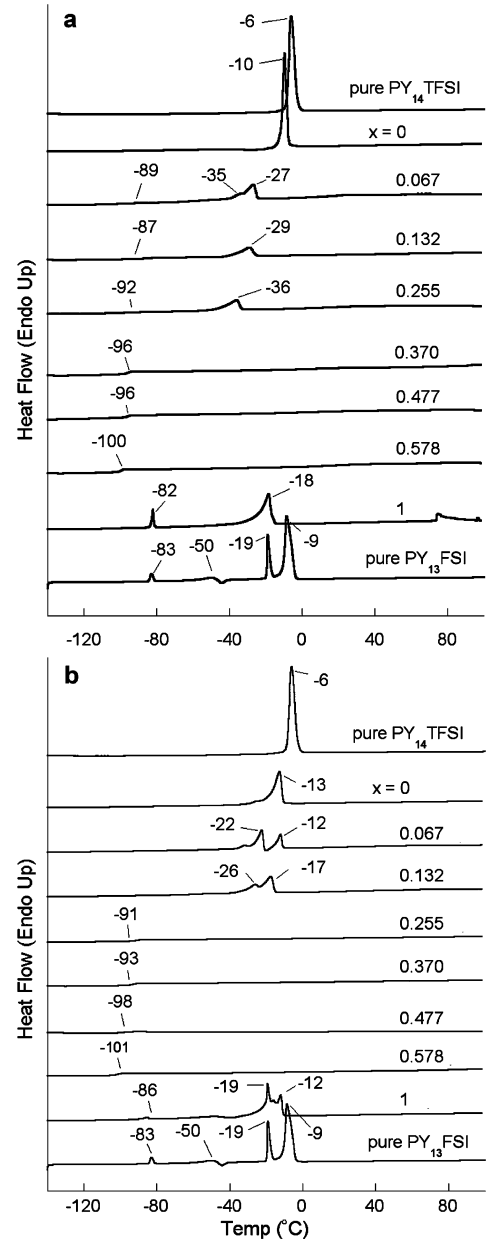

Figure 2. DSC heating traces (5 °C min^{-1}) of (1−x) $PY_{14}TFSI$-(x) $PY_{13}FSI$-0.3 M LiX mixtures: (a) $X = TFSI^-$ and (b) $X = PF_6^-$.

but this peak was not reproducible with varying crystallization procedures, suggesting the presence of a metastable (polymorphic) phase.[18] One explanation for the inconsistency of the data in Figure 1 is that a small fraction of the sample is, under certain conditions, able to crystallize into a metastable phase (not related to the other phase with its two solid−solid phase transitions) which melts near −55 °C, and immediately after melting, the liquid recrystallizes (since there is still the other solid crystalline phase present) into the thermodynamically stable phase. This behavior explains much in Figure 1. It does not, however, account for the new peak observed near −11 °C. This peak may be due to a new crystalline phase containing the $LiPF_6$ salt. It is difficult to crystallize this phase, however, and only in the last heating trace is a significant amount of this phase present.

Figure 2a shows the DSC heat traces for the $(1 - x)$ $PY_{14}TFSI-(x)PY_{13}FSI$−0.3 M LiTFSI mixtures. Pure $PY_{14}TFSI$ has a T_m of −6 °C (as well as a metastable phase with a T_m of

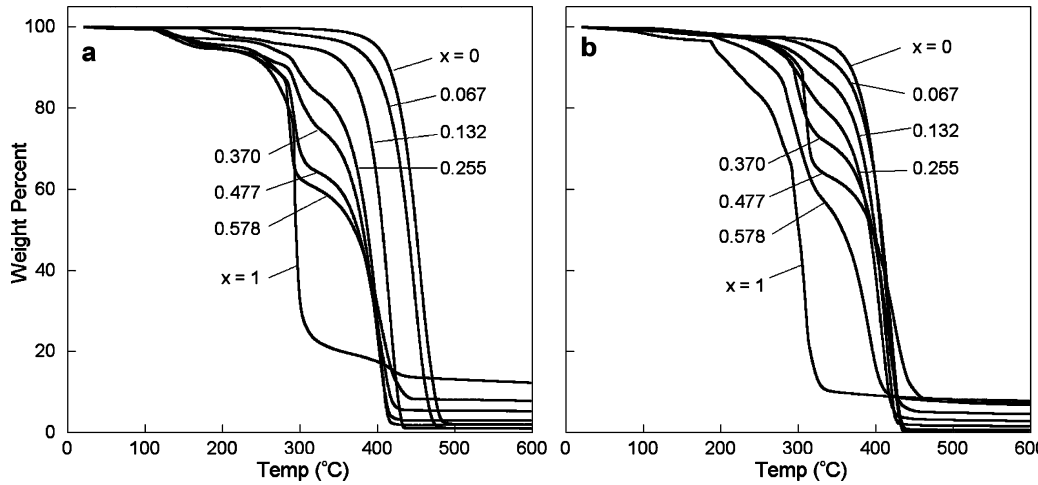

Figure 3. Variable-temperature TGA heating traces (5 °C min^{-1}) of (1−x) $PY_{14}TFSI$-(x) $PY_{13}FSI$-0.3 M LiX mixtures: (a) $X = TFSI^-$ and (b) $X = PF_6^-$ (N_2 atmosphere).

−18 °C).[16] Adding 0.3 M LiTFSI (the $x = 0$ sample) lowers the T_m of the $PY_{14}TFSI$ to −10 °C (standard liquidus behavior as the second phase containing the LiTFSI salt results in smaller $PY_{14}TFSI$ crystals). The phase diagram reported for binary $PY_{14}TFSI$−LiTFSI mixtures indicates that the phase containing the LiTFSI salt has a $2PY_{14}TFSI{\cdot}LiTFSI$ (33 mol % LiTFSI) composition for the dilute LiTFSI region of the phase diagram.[16] No peak for this phase is noted (Figure 2a), however, as the T_m of this phase for the 0.3 M LiTFSI concentration is close to that of the eutectic concentration of approximately 15 mol % LiTFSI.[16] As the $PY_{13}FSI$ mole fraction increases (x increases) in the ternary mixtures, the amount of $PY_{14}TFSI$ that may be crystallized decreases. The $x = 0.370$, 0.477, and 0.578 samples could not be crystallized despite repeated cycling at low temperature. The T_g tends to decrease with increasing fraction of $PY_{13}FSI$. For the sample containing only $PY_{13}FSI$ ($x = 1$), some of the $PY_{13}FSI$ IL is able to crystallize, but the T_m is lower than that of neat $PY_{13}FSI$ due to the presence of the 0.3 M LiTFSI salt (standard liquidus behavior). It is likely that the T_m and first solid−solid phase transition for the crystalline $PY_{13}FSI$ phase overlap, resulting in the T_m at −18 °C. There is no evidence of a new crystalline phase containing the LiTFSI salt. Rather, this salt appears to remain in an amorphous phase with some of the IL (indicated by a small T_g for the sample).

Figure 2b shows the DSC heat traces for $(1 - x)$ $PY_{14}TFSI$−$(x)PY_{13}FSI$−0.3 M $LiPF_6$ mixtures. For the $PY_{14}TFSI$-rich samples ($x = 0$, 0.067, 0.132), there are clear differences in the melting peaks from what is found for neat $PY_{14}TFSI$.[16] These differences may (at least in part) be attributed to the formation of a metastable crystalline phase that may be formed by the pure $PY_{14}TFSI$ salt (since there is a relatively small amount of the second IL),[16] as well as the presence of the 0.3 M $LiPF_6$. Once again, there is no evidence from this data that a new crystalline phase forms containing the $LiPF_6$ salt for these samples.

TGA data for the mixtures are shown in Figure 3. The $PY_{14}TFSI$−0.3 M LiTFSI sample has excellent thermal stability (the onset point for mass loss (1 wt %) is about 350 °C; Figure 3a, $x = 0$), whereas significant mass loss is observed for the $PY_{13}FSI$−0.3 M LiTFSI sample (the onset point for mass loss (1 wt %) is about 122 °C; Figure 3a, $x = 1$). As the $PY_{13}FSI$ mole fraction increases (x increases), the thermal stability of the mixtures decreases. Note that approximately 8−12 wt % of the sample mass remains after decomposition for the $x = 1$ samples, and no sample mass remains after decomposition for the $x = 0$ samples. For the $x = 0.255$, 0.370, 0.477, and 0.578 samples, a second thermal process begins near 250 °C and finishes near 450 °C. There does appear to be a delay in the thermal decomposition of the $PY_{13}FSI$ component of the mixtures (at least for these variable-temperature measurements). The mixtures with $LiPF_6$ (Figure 3b) have similar behavior to those with LiTFSI. All of the mixtures, including $PY_{14}TFSI$−$LiPF_6$ ($x = 0$), lose a small amount of mass beginning at approximately 117 °C. Although the addition of $PY_{13}FSI$ does lower the temperature for the onset of mass loss from that of the $PY_{14}TFSI$−0.3 M LiX samples, the mixed IL samples progressively decompose at a higher temperature than the $PY_{13}FSI$−0.3 M LiX samples, indicating that the ternary electrolytes may have improved safety characteristics relative to the $PY_{13}FSI$−0.3 M LiX electrolytes.

Conclusions

The addition of small amounts of $PY_{13}FSI$ to the $PY_{14}TFSI$−0.3 M LiX (X = $TFSI^-$ or PF_6^-) electrolytes substantially increases the ionic conductivity of the mixtures (relative to the binary $PY_{14}TFSI$− or $PY_{13}FSI$−0.3 M LiX mixtures) at low temperature. As shown here, the use of mixed ILs also greatly hinders the ability of the samples to crystallize. The thermal stability of the mixtures is reduced somewhat from that of $PY_{14}TFSI$−0.3 M LiX mixtures by the addition of the $PY_{13}FSI$, but it remains acceptable for Li battery applications. Thus, the use of mixed ILs with a lithium salt appears to be a promising approach to optimizing the properties of electrolytes for advanced Li batteries.

Acknowledgment. This material is based upon work supported by, or in part by, the U.S. Army Research Laboratory and the U.S. Army Research Office under Contract/Grant Number W911NF-07-1-0556. S.P. and G.B.A. also wish to thank the financial support of the European Commission within the FP6 STREP Project ILLIBAT (Contract No. NMP3-CT-2006-033181).

References and Notes

(1) Xu, K. *Chem. Rev.* **2004**, *104*, 4303.
(2) Earle, M. J.; Seddon, K. R. *Pure Appl. Chem.* **2000**, *72*, 1391.
(3) Dupont, J.; de Souza, R. F.; Suarez, P. A. Z. *Chem. Rev.* **2002**, *102*, 3667.
(4) Panozzo, S.; Armand, M.; Stephan, O. *Appl. Phys. Lett.* **2002**, *80*, 679.

(5) Wang, P.; Zakeeruddin, S. M.; Exnar, I.; Gratzel, M. *Chem. Commun.* **2002**, *24*, 2972.

(6) Fuller, J.; Breda, A. C.; Carlin, R. T. *J. Electroanal. Chem.* **1998**, *29*, 459.

(7) Nakagawa, H.; Izuchi, S.; Kunawa, K.; Nukuda, T.; Aihara, Y. *J. Electrochem. Soc.* **2003**, *150*, A695.

(8) Sakaebe, H.; Matsumoto, H. *Electrochem. Commun.* **2003**, *5*, 594.

(9) Noda, A.; Susan, M. A. B. H.; Kudo, K.; Mitsushima, S.; Hayamizu, K.; Watanabe, M. *J. Phys. Chem. B* **2003**, *107*, 4024.

(10) Balducci, A.; Henderson, W. A.; Mastragostino, M.; Passerini, S.; Simon, P.; Soavi, F. *Electrochim. Acta* **2005**, *50*, 2233.

(11) Shin, J.-H.; Henderson, W. A.; Passerini, S. *J. Electrochem. Soc.* **2005**, *152*, A978.

(12) Shin, J.-H.; Henderson, W. A.; Passerini, S. *Electrochem. Solid State Lett.* **2005**, *8*, A125.

(13) Shin, J.-H.; Henderson, W. A.; Appetecchi, G. B.; Alessandrini, F.; Passerini, S. *Electrochim. Acta* **2005**, *50*, 3859.

(14) Paulechka, Y. U.; Zaitsau, D. H.; Kabo, G. J.; Strechan, A. A. *Thermochim. Acta* **2005**, *439*, 158.

(15) Morris, R. E. *Angew. Chem., Int. Ed.* **2008**, *47*, 442.

(16) Henderson, W. A.; Passerini, S. *Chem. Mater.* **2004**, *16*, 2881.

(17) Appetecchi, G. B.; Montanino, M.; Balducci, A.; Lux, S. F.; Winter, M.; Passerini, S. *J. Power Sources.* **2009**, *192*, 599.

(18) Zhou, Q.; Henderson, W. A.; Appetecchi, G. B.; Montanino, M.; Passerini, S. *J. Phys. Chem. B* **2008**, *112*, 13577.

(19) Paillard, E.; Zhou, Q.; Henderson, W. A.; Appetecchi, G. B.; Montanino, M.; Passerini, S. *J. Electrochem. Soc.* **2009**, *156*, A891.

(20) Appetecchi, G. B.; Montanino, M.; Zane, D.; Carewska, M.; Alessandrini, F.; Passerini, S. *Electrochim. Acta* **2009**, *54*, 1325.

(21) Lux, S. F.; Schmuck, M.; Appetechi, G. B.; Passerini, S.; Winter, M.; Balducci, A. *J. Power Sources.* **2009**, *192*, 606.

JP911759D